

Learning to Efficiently Propagate for Reasoning on Knowledge Graphs

Zhaocheng Zhu*

Mila - Québec AI Institute
Université de Montréal

Xinyu Yuan*

School of EECS
Peking University

Louis-Pascal Xhonneux

Mila - Québec AI Institute
Université de Montréal

Ming Zhang

School of Computer Science
Peking University

Maxime Gazeau

LG Electronics AI Lab

Jian Tang

Mila - Québec AI Institute
HEC Montréal
CIFAR AI Chair

Abstract

Path-based methods are more appealing solutions than embedding methods for knowledge graph reasoning, due to their interpretability and generalization ability to unseen graphs. However, path-based methods usually suffer from the problem of scalability, as the time complexity grows exponentially w.r.t. the length of paths. While recent methods compute reasoning paths with the Bellman-Ford algorithm in polynomial time, the time and memory cost remains very high, as they need to propagate through all the nodes and edges in the graph. In this paper, we propose A*Net, an efficient model for path-based reasoning on knowledge graphs. Inspired by the classical A* algorithm for shortest path problems, our A*Net prioritizes important nodes and edges at each propagation step, to reduce the time and memory footprint. Unlike the classical A* algorithm that uses a heuristic function, we propose to learn the priority function for each node to capture the complex semantics in knowledge graphs. The priority function and the propagation steps are jointly optimized through backpropagation. Experiments on both transductive and inductive knowledge graph reasoning benchmarks show that A*Net achieves competitive performance with existing state-of-the-art path-based methods, and meanwhile reduces the number of messages, the time and the memory cost up to $7.2\times$, $3.4\times$ and $4.9\times$ respectively.

1 Introduction

Reasoning, the ability to apply logic to draw new conclusions from existing facts, has been long pursued as a goal of artificial intelligence [28, 17]. Knowledge graphs encapsulate facts in relational edges between entities, and serve as a foundation for reasoning. Reasoning over knowledge graphs is usually studied in the form of knowledge graph completion, where a model is asked to predict missing triplets based on observed triplets in the knowledge graph. Such a task can be used to not only populate existing knowledge graphs, but also improve downstream applications like question answering [4] and recommender systems [45].

Path-based methods are an appealing solution to knowledge graph reasoning, due to their alignment with human cognition. Take the knowledge graph in Fig. 1(a) as an example, we can easily prove that $Mother(a, f)$ holds, because there are two paths $a \xrightarrow{Father} b \xrightarrow{Wife} f$ and $a \xleftarrow{Brother} c \xrightarrow{Mother} f$. Traditionally, such reasoning paths are generated by logic inference algorithms [26] that search and combine basic

*Equal contribution. This work was done when Xinyu Yuan was an intern at Mila.

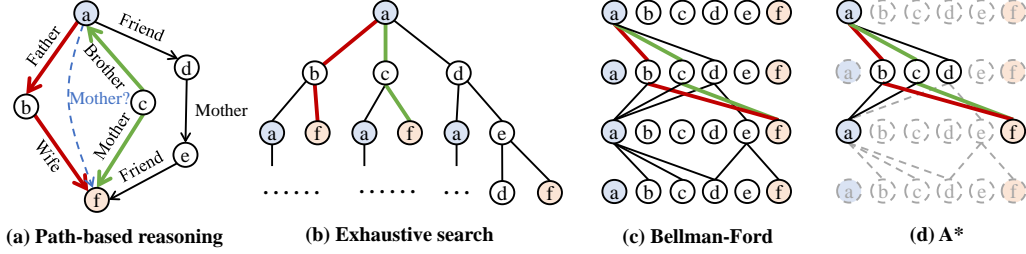


Figure 1: Illustration of A*Net. **(a)** Given a query, only a few important paths (showed in colors) are necessary for reasoning. Note that paths can go in the reverse direction of relations. **(b)** Exhaustive search algorithm (e.g., Path-RNN, PathCon) enumerates all paths in exponential time. **(c)** Bellman-Ford algorithm (e.g., NeuralLP, DRUM, NBFNet, RED-GNN) computes all paths in polynomial time, but needs to propagate through all nodes and edges. **(d)** A*Net learns a priority function to select a subset of nodes and edges at each propagation step, and avoids exploring all nodes and edges.

paths according to handcrafted logic rules. Recently, there is a surge of methods [27, 9, 38, 49] that directly learn representations of paths for reasoning on knowledge graphs.

However, the number of paths grows exponentially w.r.t. the path length, which imposes a huge challenge for applying path-based methods to real-world knowledge graphs. Therefore, it is necessary to develop techniques that reduce the time and memory cost of path-based methods. Recently, several works [43, 30, 49, 46] assume that the common prefix of paths can be factorized out, and apply the Bellman-Ford algorithm to learn path representations in polynomial time. Despite the good performance of these methods, the Bellman-Ford algorithm needs to propagate through the whole knowledge graph, which is still a restriction for their application on large graphs.

In this paper, we propose A*Net, an efficient graph neural network (GNN) model for path-based reasoning. Our method is motivated by the A* algorithm [19] for shortest-path problems, which extends the Bellman-Ford algorithm with a priority function to guide the search towards better paths for a given goal. Inspired by the design of A* algorithm, given a head entity h and a query relation q , we compute a priority score for each entity to guide the propagation towards more important paths for reasoning. At each iteration step, we select K nodes and L edges according to their priority, and propagate their representations to update the nodes in their neighborhood. Unlike the A* algorithm that uses a handcrafted heuristic function to compute the priority, we design a neural priority function based on aggregated path representations of each node. The neural priority function is jointly optimized with path-based reasoning to capture the complex relation semantics in knowledge graphs.

We evaluate our method on 2 standard knowledge graph reasoning datasets in both transductive and inductive settings. We also visualize the paths learned by A*Net. The contributions of this paper are:

- We provide a definition of important paths in path-based methods. We show that the representation over important paths can be recursively computed via the A* algorithm (Sec. 3.1).
- We propose A*Net with a neural priority function that is aligned with the intuition of the A* algorithm (Sec. 3.2). By jointly learning the priority function with path-based reasoning, A*Net achieves better performance than handcrafted priority functions (Sec. 4.3).
- A*Net achieves competitive performance with existing state-of-the-art path-based methods, and significantly reduces the number of messages, the time and the memory cost (Sec. 4.2).
- Visualization of paths shows that A*Net can capture important paths for reasoning (Sec. 4.4).

2 Preliminary

Knowledge Graph Reasoning A knowledge graph $\mathcal{G} = (\mathcal{V}, \mathcal{E}, \mathcal{R})$ is composed of finite sets of entities \mathcal{V} , facts \mathcal{E} and relation types \mathcal{R} . Each fact is a triplet $(x, r, y) \in \mathcal{V} \times \mathcal{R} \times \mathcal{V}$, which indicates the presence of relation r from entity x to entity y . The task of knowledge graph reasoning aims at predicting answers for queries like $(u, q, ?)$ or $(?, q, u)$ in a knowledge graph. Without loss of generality, we assume the query is $(u, q, ?)$, since $(?, q, u)$ can always be reformulated as $(u, q^{-1}, ?)$

with q^{-1} being the inverse relation of q . Given a query $(u, q, ?)$, we need to predict the set of all entities $\mathcal{V}_{(u,q,?)}$, such that $\forall v \in \mathcal{V}_{(u,q,?)}$ the fact (u, q, v) should be true.

Path-based Methods Path-based methods solve knowledge graph reasoning by looking at the paths between a pair of entities in the knowledge graph. For example, a path $a \xrightarrow{\text{Father}} b \xrightarrow{\text{Wife}} f$ may be used to predict $\text{Mother}(a, f)$ in Fig. 1(a). From a representation learning perspective, path-based methods first compute the representation $\mathbf{h}_q(P)$ for each path P , and then aggregate the set of paths $\mathcal{P}_{u \rightsquigarrow v}$ from entity u to entity v to predict the triplet. Formally, the representation $\mathbf{h}_q(u, v)$ for a triplet (u, q, v) is computed by

$$\mathbf{h}_q(u, v) = \bigoplus_{P \in \mathcal{P}_{u \rightsquigarrow v}} \mathbf{h}_q(P) = \bigoplus_{P \in \mathcal{P}_{u \rightsquigarrow v}} \bigotimes_{(x,r,y) \in P} \mathbf{w}_q(x, r, y) \quad (1)$$

where \bigoplus is a permutation-invariant aggregation function over paths, and \bigotimes may be a permutation-sensitive aggregation function over edges. Different choices for \bigoplus and \bigotimes recover many classical path-based methods, such as shortest path problems ($\bigoplus = \min$, $\bigotimes = \sum$) and personalized PageRank ($\bigoplus = \sum$, $\bigotimes = \prod$) [49]. However, it is hard to directly solve path-based methods through Eqn. 1, since the number of paths usually grows exponentially w.r.t. the path length.

Path-based Reasoning with Bellman-Ford algorithm Given that shortest path problems are a special case of path-based methods, recent works [43, 30, 49, 46] show that path-based methods can be solved by the Bellman-Ford algorithm [3]. By assuming that \bigotimes is distributive over \bigoplus ², we can extract the common prefix of different paths, and apply dynamic programming to compute path-based methods in polynomial time. Specifically, the Bellman-Ford algorithm applied to knowledge graphs iteratively computes $\mathbf{h}_q^{(t)}(u, v)$ by aggregating messages from $\mathcal{E}(v)$, the neighborhood of node v

$$\mathbf{h}_q^{(0)}(u, v) \leftarrow \mathbb{1}_q(u = v) \quad (2)$$

$$\mathbf{h}_q^{(t)}(u, v) \leftarrow \left(\bigoplus_{(x,r,v) \in \mathcal{E}(v)} \mathbf{h}_q^{(t-1)}(u, x) \otimes \mathbf{w}_q(x, r, v) \right) \oplus \mathbf{h}_q^{(0)}(u, v) \quad (3)$$

where $\mathbb{1}_q$ is an indicator function to initialize the boundary condition for Bellman-Ford algorithm (e.g., $\mathbf{h}_q^{(0)}(u, v) = \begin{cases} 0 & u = v \\ +\infty & u \neq v \end{cases}$ in the case of shortest path problems). Despite the polynomial time complexity achieved by the Bellman-Ford algorithm, Eqn. 3 still needs to visit $|\mathcal{V}|$ nodes and $|\mathcal{E}|$ edges to compute $\mathbf{h}_q^{(t)}(u, v)$ for all $v \in \mathcal{V}$, which is not feasible for large knowledge graphs.

A* Algorithm A* algorithm [19] is an extension of the Bellman-Ford algorithm for shortest path problems. The A* algorithm defines a priority function for each node based on a heuristic function specified by the user, and prioritizes propagation through nodes with higher priority. With an appropriate heuristic function, A* algorithm can reduce the search space of the Bellman-Ford algorithm. Formally, using the same notation as Eqn. 1, the priority function for node x is

$$s(x) = d(u, x) \otimes g(x, v) \quad (4)$$

where $d(u, x)$ is the length of current shortest path from u to x , and $g(x, v)$ is a heuristic function estimating the cost from x to the target node v . For instance, for the shortest path problem in a grid world (Fig. 2), $g(x, v)$ is usually defined as the L_1 distance from x to v . In this case, \otimes is the addition operator and $s(x)$ becomes a lower bound for the shortest path length from u to v through x . During each iteration, we prioritize propagation through nodes with smaller $s(x)$.

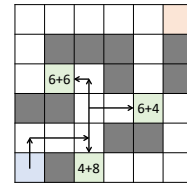


Figure 2: Illustration of A* algorithm in a grid-world shortest path problem. Each green block is labeled with its current shortest path length plus the heuristic value. A* will prioritize the block with $6 + 4$.

²More precisely, $\langle \bigoplus, \bigotimes \rangle$ forms a semiring system [20].

3 Proposed Method

In this section, we present a novel model A*Net to efficiently solve path-based methods based on A* algorithm. We first show that A* algorithm can be naturally derived from the observation that not every path has the same importance for reasoning (Sec. 3.1). Then we propose A*Net to learn the priority function together with path-based reasoning on knowledge graphs (Sec. 3.2).

3.1 Path-based Reasoning with A* Algorithm

As discussed in Sec. 2, the drawback of the Bellman-Ford algorithm is that it needs to visit all $|\mathcal{V}|$ nodes and $|\mathcal{E}|$ edges to compute path-based methods over the space of all possible paths. However, in real-world knowledge graphs, only a small portion of paths are related to the query. Based on this observation, we introduce the concept of important paths. We then show that the representations of important paths can be iteratively computed with the A* algorithm under mild assumptions.

Important Paths for Reasoning Given a query relation and a pair of entities, only some of the paths between the entities are important for answering the query. Consider the example in Fig. 1(a), the path $a \xrightarrow{\text{Friend}} d \xrightarrow{\text{Mother}} e \xrightarrow{\text{Friend}} f$ cannot determine whether f is an answer to $\text{Mother}(a, ?)$. On the other hand, kinship paths like $a \xrightarrow{\text{Father}} b \xrightarrow{\text{Wife}} f$ or $a \xleftarrow{\text{Brother}} c \xrightarrow{\text{Mother}} f$ are able to predict that $\text{Mother}(a, f)$ is true. Formally, we define $\mathcal{P}_{u \rightsquigarrow v|q} \subseteq \mathcal{P}_{u \rightsquigarrow v}$ to be the set of paths from u to v that is important to the query relation q . Mathematically, we can express this as

$$h_q(u, v) = \bigoplus_{P \in \mathcal{P}_{u \rightsquigarrow v}} h_q(P) \approx \bigoplus_{P \in \mathcal{P}_{u \rightsquigarrow v|q}} h_q(P) \quad (5)$$

In other words, any path $P \in \mathcal{P}_{u \rightsquigarrow v} \setminus \mathcal{P}_{u \rightsquigarrow v|q}$ has negligible contribution to the representation $h_q(u, v)$. In real-world knowledge graphs, the number of important paths $|\mathcal{P}_{u \rightsquigarrow v|q}|$ may be several orders of magnitudes smaller than the number of paths $|\mathcal{P}_{u \rightsquigarrow v}|$. If we compute the representation $h_q(u, v)$ using only the important paths, we can accelerate path-based reasoning.

Iterative Computation of Important Paths To accelerate path-based reasoning, we need to discover the set of important paths $\mathcal{P}_{u \rightsquigarrow v|q}$ for a given u, q and all $v \in \mathcal{V}$. However, it is hard to directly extract important paths from $\mathcal{P}_{u \rightsquigarrow v}$, since the size of $\mathcal{P}_{u \rightsquigarrow v}$ is exponentially large. In fact, the paths in $\mathcal{P}_{u \rightsquigarrow v}$ form a tree structure (Fig. 3), and we show an efficient way to extract the important paths on the tree. Notice that we can determine whether a path is not important if any prefix of this path is not important for the query. We assume the existence of a binary path function $m_q : \mathcal{P} \mapsto \{0, 1\}$ that determines whether a set of paths contains any important path for relation q , by looking at their shared prefix path P . We can use $m_q(P)$ to iteratively construct a slightly larger superset of important paths (see App. A for proofs). Let $\hat{\mathcal{P}}_{u \rightsquigarrow v|q}^{(t)} \supseteq \mathcal{P}_{u \rightsquigarrow v|q}^{(t)}$ denote the superset of important paths of length t , we have the following iterations (Fig. 3)

$$\hat{\mathcal{P}}_{u \rightsquigarrow v|q}^{(0)} \leftarrow \{(u, \text{self loop}, v)\} \text{ if } u = v \text{ else } \emptyset \quad (6)$$

$$\hat{\mathcal{P}}_{u \rightsquigarrow v|q}^{(t)} \leftarrow \bigcup_{(x, r, v) \in \mathcal{E}(v)} \left\{ \text{concat}(P, \{(x, r, v)\}) \mid P \in \hat{\mathcal{P}}_{u \rightsquigarrow x|q}^{(t-1)}, m_q(P) = 1 \right\} \quad (7)$$

where $\text{concat}(\cdot, \cdot)$ concatenates two paths. We prove the correctness of Eqn. 6 and 7 in App. A. We further assume that paths with the same length and the same stop node can be merged, similar to the case in the Bellman-Ford algorithm. Therefore, Eqn. 7 can be rewritten as

$$\hat{\mathcal{P}}_{u \rightsquigarrow v|q}^{(t)} \leftarrow \bigcup_{x \in \mathcal{V}, s_{uq}^{(t-1)}(x)=1, (x, r, v) \in \mathcal{E}(v)} \left\{ \text{concat}(P, \{(x, r, v)\}) \mid P \in \hat{\mathcal{P}}_{u \rightsquigarrow x|q}^{(t-1)} \right\} \quad (8)$$

where $s_{uq} : \mathcal{V} \mapsto \{0, 1\}$ measures whether there is an important path from node u to node x .

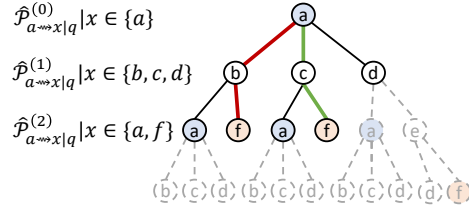


Figure 3: The colored paths are important paths $\mathcal{P}_{u \rightsquigarrow v|q}$, while the solid paths are the superset $\hat{\mathcal{P}}_{u \rightsquigarrow v|q}$ used in Eqn. 7.

Reasoning with A* Algorithm The above iteration (Eqn. 8) computes the set of important paths. Now we show how to use it to compute the representation $\mathbf{h}_q(u, v)$ in path-based methods. To do this, we substitute Eqn. 8 for Eqn. 3, and arrive at the A* iteration (Fig. 1(d))

$$\mathbf{h}_q^{(t)}(u, v) \leftarrow \left(\bigoplus_{x \in \mathcal{V}, s_{uq}^{(t-1)}(x)=1, (x, r, v) \in \mathcal{E}(v)} \mathbf{h}_q^{(t-1)}(u, x) \otimes \mathbf{w}_q(x, r, v) \right) \oplus \mathbf{h}_q^{(0)}(u, v) \quad (9)$$

Note the A* algorithm uses the same boundary condition as Eqn. 2. Since we only care about path-based reasoning, we do not need to explicitly compute the set of paths $\hat{\mathcal{P}}_{u \rightsquigarrow v|q}^{(t)}$. In Eqn. 9, the node function $s_{uq}(x)$ serves as a (hard) priority to select nodes for propagation. Since we do not have an oracle for function $s_{uq}(x)$, we need to design a (soft) priority function for the A* algorithm.

3.2 Path-based Reasoning with A*Net

Both the performance and the efficiency of the A* algorithm heavily rely on the heuristic function. While it is straightforward to use L_1 distance as the heuristic function for grid-world shortest path problems, it is not clear what a good priority function for knowledge graph reasoning is, due to the complex relation semantics in knowledge graphs. In this section, we discuss a neural priority function, which can be jointly learned with path-based reasoning.

Neural Priority Function To design a neural priority function, we draw inspiration from the priority function in the classical A* algorithm for shortest path problems (Eqn. 4). The priority function has two terms, $d(u, x)$ and $g(x, v)$. Intuitively, $d(u, x)$ measures the current distance between node u and x , and $g(x, v)$ estimates the remaining distance from node x to v . In knowledge graph reasoning, when we compute the priority function $s_{uq}^{(t)}(x)$ at step t , we can replace $d^{(t)}(u, x)$ with the current representation $\mathbf{h}_q^{(t)}(u, x)$. However, it is challenging to find a counterpart of $g^{(t)}(x, v)$ in knowledge graph reasoning, since we do not know the answer entity v beforehand. Instead, we approximate the term $g^{(t)}(x, v)$ with another function $g^{(t)}(u, x, q)$, because we should be able to predict any answer entity v given u and q . Specifically, we parameterize $s_{uq}(x)$ as the follows

$$s_{uq}^{(t)}(x) = d^{(t)}(u, x) \otimes g^{(t)}(u, x, q) = \mathbf{h}_q^{(t)}(u, x) \otimes g([\mathbf{h}_q^{(t)}(u, x), \mathbf{q}]) \quad (10)$$

where $g(\cdot)$ is a feed-forward network and $[\cdot, \cdot]$ concatenates two representations. Since the \otimes outputs a vector representation, we further use a feed-forward network followed by a sigmoid function to map $s_{uq}^{(t)}(x)$ to $[0, 1]$. To apply the priority function to select nodes in the A* algorithm (Eqn. 9), we simply pick the top- K nodes according to the current priority function $s_{uq}^{(t)}(x)$ for $x \in \mathcal{V}$.

Learning In order to learn the neural priority function for path-based reasoning, we incorporate the neural priority function as a weight for each message in the A* iteration

$$\mathbf{h}_q^{(t)}(u, v) \leftarrow \left(\bigoplus_{x \in \mathcal{X}^{(t)}, (x, r, v) \in \mathcal{E}(v)} s_{uq}^{(t-1)}(x) \left(\mathbf{h}_q^{(t-1)}(u, x) \otimes \mathbf{w}_q(x, r, v) \right) \right) \oplus \mathbf{h}_q^{(0)}(u, v) \quad (11)$$

where $\mathcal{X}^{(t)}$ denotes the set of top- K nodes prioritized by $s_{uq}^{(t)}(x)$. Eqn. 11 encourages the model to learn larger weights $s_{uq}^{(t)}(x)$ for nodes that are important for the reasoning task. A pseudo code of A*Net is illustrated in Alg. 1. In practice, since some nodes may have very large degrees, we further select top- L edges of the neighborhood of $\mathcal{X}^{(t)}$ in A* iteration. See App. B for more details.

Nevertheless, it is still too challenging to train the neural priority function, since we do not know the ground truth for important paths, and there is no direct supervision for the priority function. Our solution is to share the weights between the priority function and the predictor for the reasoning task. The intuition is that the reasoning task can be viewed as a weak supervision for the priority function. Recall that the goal of $s_{uq}^{(t)}(x)$ is to determine whether there exists an important path from u to x (Eqn. 8). In the reasoning task, any positive answer entity must be present on at least one important path, while negative answer entities are less likely to be on important paths. By sharing the weights between the priority function and the reasoning predictor, we can improve the convergence

of the neural priority function. Our ablation study suggests this trick is essential for training A*Net (Tab. 4b). The whole model is trained to minimize the binary cross entropy loss over triplets [33]

$$\mathcal{L} = -\log p(u, q, v) - \sum_{i=1}^n \frac{1}{n} \log(1 - p(u'_i, q, v'_i)) \quad (12)$$

where (u, q, v) is the positive sample and $\{(u'_i, q, v'_i)\}_{i=1}^n$ are the negative samples. Each negative sample (u_i, q, v_i) is generated by corrupting either the head or the tail entity in a positive sample.

Efficient Implementation with Padding-Free Operations

Modern neural networks heavily relies on batched execution to unleash the power of GPUs for parallel computation. While Alg. 1 is easy to implement for a single positive sample and its negative samples that share the same u and q , it is not trivial to batch A*Net for multiple positive samples. The challenge is that different samples may have very different sizes for nodes $\mathcal{V}^{(t)}$ and edges $\mathcal{E}^{(t)}$. A common approach is to pad the set of nodes or edges to a predefined constant, which would counteract the acceleration brought by A*Net.

Here we introduce padding-free operations to avoid the overhead in batched execution. Specifically, we implement padding-free version of *topk* and *unique* operations, where *unique* is needed for the union operation in Alg. 1. The high-level idea is to convert batched execution of different small samples into the execution of a single large sample, which can be paralleled by existing operations in deep learning frameworks. For example, the batched execution of *topk*([[1, 3], [2, 1, 0]]) can be converted into a sorting problem over [1+0, 3+0, 2+4, 1+4, 0+4] by adding 0 and 4 as offsets for two samples respectively. See App. C for a detailed discussion of the padding-free operations.

4 Experiments

We evaluate A*Net on standard transductive and inductive knowledge graph reasoning datasets. Besides, we conduct several ablation studies to verify our design choices, and reveal the performance-efficiency trade-off. We also visualize the important paths learned by the priority function in A*Net.

4.1 Experiment Setup

Datasets & Evaluation We evaluate A*Net on two standard knowledge graphs, FB15k-237 [35] and WN18RR [13]. For the transductive setting, we use the standard splits from their original works [35, 13]. For the inductive setting, we use the splits provided by [34], which contains 4 different split versions for each dataset. As for evaluation, we follow the standard filtered ranking protocol [5] for knowledge graph reasoning. We measure the performance with mean reciprocal rank (MRR) and HITS at K (H@K). The efficiency is measured by the average number of messages (#message) per layer, wall time per epoch and memory cost. See more details in App. D.

Implementation Details Our work is developed based on the open-source codebase of path-based reasoning with Bellman-Ford algorithm³. For a fair comparison with existing path-based methods, we follow the implementation of NBFNet [49] and parameterize \oplus with principal neighborhood aggregation (PNA) [10], and parameterize \otimes with the relation operation from DistMult [42], i.e., vector multiplication. The indicator function (Eqn. 2) $\mathbb{1}_q(u = v) = \mathbb{1}(u = v)\mathbf{q}$ is parameterized with a query embedding \mathbf{q} , and the edge representation (Eqn. 11) $\mathbf{w}_q(x, r, v) = \mathbf{W}_r\mathbf{q} + \mathbf{b}_r$ is parameterized

Algorithm 1 A*Net

Input: head entity u , query relation q , #iterations T

Output: $p(v|u, q)$ for all $v \in \mathcal{V}$

```

1: for  $v \in \mathcal{V}$  do                                ▷ Initialization
2:    $\mathbf{h}_q^{(0)}(u, v) \leftarrow \mathbb{1}_q(u = v)$ 
3: end for
4: for  $t \leftarrow 1$  to  $T$  do                            ▷ A* iteration
5:   ▷ Generate prioritized subsets of nodes
6:    $\mathcal{X}^{(t)} \leftarrow \text{TOPK}(s_{uq}^{(t-1)}(x)|x \in \mathcal{V})$ 
7:   ▷ Generate prioritized subsets of edges
8:    $\mathcal{E}^{(t)} \leftarrow \bigcup_{x \in \mathcal{X}^{(t)}} \mathcal{E}(x)$ 
9:    $\mathcal{E}^{(t)} \leftarrow \text{TOPL}(s_{uq}^{(t-1)}(v)|(x, r, v) \in \mathcal{E}^{(t)})$ 
10:   $\mathcal{V}^{(t)} \leftarrow \bigcup_{(x, r, v) \in \mathcal{E}^{(t)}} \{v\}$ 
11:  for  $v \in \mathcal{V}^{(t)}$  do
12:    Compute  $\mathbf{h}_q^{(t)}(u, v)$  with Eqn. 11
13:    Compute priority  $s_{uq}^{(t)}(v)$  with Eqn. 10
14:  end for
15: end for
16: ▷ Share weights between  $s_{uq}(v)$  and the predictor
17: return  $s_{uq}^{(T)}(v)$  as  $p(v|u, q)$  for all  $v \in \mathcal{V}$ 

```

³<https://github.com/DeepGraphLearning/NBFNet>. MIT license.

as a linear function over the query relation q for FB15k-237 and an embedding $w_q(x, r, v) = r$ for WN18RR. We use the same preprocessing steps as in [49], including augmenting each triplet with a flipped triplet, and dropping out edges that directly connect query entities during training.

For the neural priority function, we have two hyperparameters: K for the maximum number of nodes and L for the maximum number of edges. To make hyperparameter tuning easier for datasets of different sizes, we define the expected degree $D = L/K$ and search the ratios $K/|\mathcal{V}|$ and $D|\mathcal{V}|/|\mathcal{E}|$ for each dataset. The other hyperparameters are kept the same as the values in [49]. We train A*Net with 4 Tesla V100 GPUs, and select the best model checkpoint based on the performance on the validation set. More implementation details and the hyperparameters can be found in App. E.

Baselines We compare A*Net against embedding methods, GNNs and path-based methods. The embedding methods include TransE [5], RotatE [33], HAKE [47], RotH [6] and ConE [2]. The GNN methods include RGCN [31], CompGCN [37] and GraIL [34]. The path-based methods include NeuralLP [43], DRUM [30] and NBFNet [49]. Note the original implementation of NBFNet not only computes representations for paths in Eqn. 1, but also considers additional paths from node x to v when computing the representation for $h_q(u, v)$ (see App. F for further discussions). For a fair comparison, we re-implement NBFNet to compute only the paths in Eqn. 1 and Fig. 1(c). We distinguish two versions with NBFNet (path+) and NBFNet (path) in our results.

4.2 Main Results

Tab. 1 summarizes the performance results on transductive knowledge graph reasoning. A*Net significantly outperforms all embedding methods and GNNs, and achieves competitive performance with NBFNet [49]. Notably, unlike NBFNet that propagates through all nodes and edges, A*Net propagates through a subset of nodes and edges selected by the neural priority function. A*Net only propagates through 10% nodes on FB15k-237 and 1% nodes on WN18RR, which suggests that most nodes and edges are not important in path-based reasoning. As showed in Tab. 2, A*Net significantly reduces the number of messages by $7.2\times$ and $5.3\times$ compared to NBFNet (path) on two datasets respectively. In addition, it also reduces the wall time for each epoch and memory cost.

Table 1: Performance on transductive knowledge graph reasoning. Results of embedding methods are taken from [2]. Results of GNNs and path-based methods are taken from [49]. For A*Net, node ratio $K/|\mathcal{V}|$ is set to 10% for FB15k-237 and 1% for WN18RR, and degree ratio $D|\mathcal{V}|/|\mathcal{E}|$ is set to 100% for both datasets. Best results are in **bold**, second best results are underlined.

Method	FB15k-237				WN18RR			
	MRR	H@1	H@3	H@10	MRR	H@1	H@3	H@10
TransE [5]	0.294	-	-	0.465	0.226	-	-	0.501
RotatE [33]	0.338	0.241	0.375	<u>0.553</u>	0.476	0.428	0.492	0.571
HAKE [47]	0.346	0.250	0.381	0.542	0.497	<u>0.452</u>	0.516	0.582
RotH [6]	0.344	0.246	0.380	0.535	0.495	0.449	0.514	0.586
ConE [2]	0.345	0.247	0.381	0.540	0.496	<u>0.453</u>	0.515	0.579
RGCN [31]	0.273	0.182	0.303	0.456	0.402	0.345	0.437	0.494
CompGCN [37]	<u>0.355</u>	<u>0.264</u>	<u>0.390</u>	0.535	0.479	0.443	0.494	0.546
NeuralLP [43]	0.240	-	-	0.362	0.435	0.371	0.434	0.566
DRUM [30]	0.343	0.255	0.378	0.516	0.486	0.425	0.513	0.586
NBFNet (path+) [49]	0.415	0.321	0.454	0.599	0.551	0.497	0.573	0.666
NBFNet (path)	0.409	0.315	0.447	0.593	0.547	0.495	0.569	<u>0.651</u>
A*Net	0.412	0.320	0.452	0.590	<u>0.538</u>	0.490	<u>0.558</u>	0.636

Table 2: Efficiency on transductive knowledge graph reasoning.

Method	FB15k-237			WN18RR		
	#message	time	memory	#message	time	memory
NBFNet (path)	315,931	56.7 min	24.7 GiB	4,824	3.57 min	24.9 GiB
A*Net	43,727	16.8 min	16.7 GiB	910	1.91 min	4.4 GiB
Improvement	$7.2\times$	$3.4\times$	$1.5\times$	$5.3\times$	$1.9\times$	$4.9\times$

Table 3: Performance on inductive knowledge graph reasoning (H@10). V1-v4 refer to the 4 standard inductive splits. Results of compared methods are taken from [49]. See App. E for node ratio $K/|\mathcal{V}|$ and degree ratio $D|\mathcal{V}|/|\mathcal{E}|$ of each split. Best results are in **bold**, second best results are underlined.

Method	FB15k-237				WN18RR			
	v1	v2	v3	v4	v1	v2	v3	v4
NeuralLP [43]	0.529	0.589	0.529	0.559	0.744	0.689	0.462	0.671
DRUM [30]	0.529	0.587	0.529	0.559	0.744	0.689	0.462	0.671
GraIL [34]	0.642	0.818	0.828	0.893	0.825	0.787	0.584	0.734
NBFNet (path+) [49]	0.834	0.949	0.951	0.960	0.948	0.905	0.893	0.890
NBFNet (path)	0.697	<u>0.871</u>	<u>0.910</u>	<u>0.907</u>	<u>0.877</u>	0.822	<u>0.720</u>	<u>0.802</u>
A*Net	<u>0.730</u>	<u>0.873</u>	<u>0.904</u>	<u>0.914</u>	<u>0.877</u>	<u>0.835</u>	<u>0.723</u>	<u>0.796</u>

Tab. 3 shows the performance results on inductive knowledge graph reasoning. We observe that A*Net outperforms all methods except NBFNet (path+). However, this is not a weakness of A*Net, since A*Net can match the performance of NBFNet (path). In fact, the gap between NBFNet (path+) and NBFNet (path) indicates that the additional paths considered in NBFNet (path+) (see App. F) contribute to the performance in the inductive setting. We leave the integration of such additional paths in A*Net as future work. Efficiency results of inductive setting are included in App. G.

4.3 Ablation Studies

Priority Function We consider two handcrafted priority functions: personalized PageRank (PPR) and Degree. PPR selects nodes with higher PPR score w.r.t. the query head entity u , while Degree selects nodes with larger degrees. Tab. 4a shows that both PPR and Degree decrease the performance compared to NBFNet (path), since they cannot capture the complex relation semantics in knowledge graphs. By comparison, our neural priority function can match the performance of NBFNet (path).

Sharing Weights As discussed in Sec. 3.2, we share the weights between the neural priority function and the reasoning predictor to help train the neural priority function. Tab. 4b compares A*Net trained with and without sharing weights. It can be observed that sharing weights is essential to train a good neural priority function in A*Net.

Trade-off between Performance and Efficiency One may change the ratios $K/|\mathcal{V}|$ and $D|\mathcal{V}|/|\mathcal{E}|$ to trade off between performance and efficiency in A*Net. Fig. 5 plots curves of the performance and the improvement of #message w.r.t. different $K/|\mathcal{V}|$ and $D|\mathcal{V}|/|\mathcal{E}|$. If we can accept a performance similar to embedding methods (e.g., ConE [2]), we can set either $K/|\mathcal{V}|$ to 2% or $D|\mathcal{V}|/|\mathcal{E}|$ to 10%, resulting in more than $60\times$ improvement in #message.

Table 4: Ablation studies of A*Net on transductive FB15k-237 ($K/|\mathcal{V}| = 10\%$, $D|\mathcal{V}|/|\mathcal{E}| = 100\%$).

(a) Choices of priority function.					(b) W/ or w/o sharing weights.				
Priority Function	MRR	FB15k-237			Share Weights	MRR	FB15k-237		
		H@1	H@3	H@10			H@1	H@3	H@10
NBFNet (path)	0.409	0.315	0.447	0.593	No	0.374	0.282	0.413	0.557
PPR	0.266	0.212	0.296	0.371	Yes	0.412	0.320	0.452	0.590
Degree	0.347	0.268	0.383	0.501					
Neural	0.412	0.320	0.452	0.590					

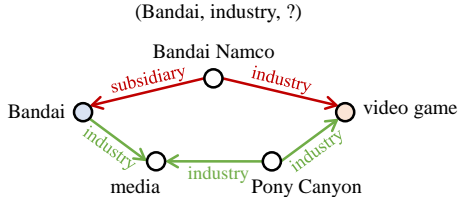


Figure 4: Visualization of important paths learned by the neural priority function in A*Net.

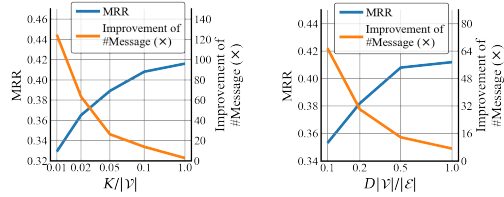


Figure 5: Performance and efficiency trade-off w.r.t. node ratio $K/|\mathcal{V}|$ and degree ratio $D|\mathcal{V}|/|\mathcal{E}|$.

4.4 Visualization of Learned Important Paths

One advantage of A*Net is that we can extract the important paths from the neural priority function. For a given query $(u, q, ?)$ and a predicted entity v , we can use the priority $s_{uq}^{(t)}(x)$ of each node in each layer to estimate the importance of a path. Empirically, the importance of a path is estimated by

$$m_q(P) = \frac{1}{|P|} \sum_{t=1, P^{(t)}=(x,r,y)}^{|P|} \frac{s_{uq}^{(t-1)}(x)}{S_{uq}^{(t-1)}} \quad (13)$$

where $S_{uq}^{(t-1)} = \max_{x \in \mathcal{V}^{(t-1)}} s_{uq}^{(t-1)}(x)$ is a normalizer to normalize the priority score for each step t . To extract the important paths with large $m_q(P)$, we perform beam search over the priority function $s_{uq}^{(t-1)}(x)$ of each layer. Fig. 4 shows the important paths learned by A*Net for a test sample in FB15k-237. Given the query $(Bandai, industry, ?)$, we can see both paths $Bandai \xleftarrow{subsidiary} Bandai \xrightarrow{industry} video\ game$ and $Bandai \xrightarrow{industry} media \xleftarrow{industry} Pony\ Canyon \xrightarrow{industry} video\ game$ are consistent with human cognition. More visualization results can be found in App. H.

5 Related Work

Path-based Reasoning Path-based methods learn to extract or combine paths for knowledge graph reasoning. Early methods like Path Ranking [24, 16] collect relational paths between entities as symbolic features, and learn a classifier to predict the triplet. Path-RNN [27, 12] and PathCon [38] improve Path Ranking by learning the representations of paths with recurrent neural networks (RNN). However, these works operate on the full set of paths between two entities, which grows exponentially w.r.t. the path length. Typically, these methods can only extract paths with at most 3 edges.

To avoid the exhaustive search of exponential number of paths, many methods learn to sample important paths for reasoning. DeepPath [40] and MINERVA [11] learn an agent to collect meaningful paths on the knowledge graph through reinforcement learning. These methods are hard to train due to the extremely sparse rewards for the paths. Later works mitigate such an issue by engineering the reward function [25], the search strategy [32], or separating the agents for positive and negative paths [21]. Other methods [9, 29] use a variational formulation to learn a sparse prior for path sampling. Another category of methods utilize the dynamic programming to search exponential number of paths in a polynomial time. NeuralLP [43] and DRUM [30] use dynamic programming to learn linear combination of logic rules. All-Paths [36] adopt a Floyd-like algorithm to learn path representations between all pairs of entities. Recently, NBFNet [49] and RED-GNN [46] leverage a Bellman-Ford-like algorithm to learn path representations from a single-source entity to all entities. While dynamic programming methods achieve state-of-the-art results among path-based methods, they still need to perform message passing on the full knowledge graph. By comparison, our A*Net learns a priority function and only explores a subset of paths, which is more efficient.

Efficient Graph Neural Networks Our work is also related to efficient graph neural networks, since both try to improve the efficiency and scalability of graph neural networks (GNNs). Sampling methods [18, 7, 22, 44] reduce the cost of message passing by computing GNNs with a sampled subset of nodes and edges. Non-parametric GNNs [23, 39, 15, 8] decouple feature propagation from feature transformation, and reduce time complexity by preprocessing the feature propagation. However, both sampling methods and non-parametric GNNs are designed for homogeneous graphs, and it is not straightforward to adapt them to knowledge graphs with complex relation semantics. On knowledge graphs, RS-GCN [14] uses reinforcement learning to learn the neighborhood sampling in RGCN [31]. DPMPN [41] learns an attention to iteratively select nodes for message passing. SQALER [1] first predicts important path types based on the query, and then applies GNNs for reasoning on the subgraph containing the paths. Our A*Net shares the same goal with these methods, but learns a neural priority function to efficiently compute path-based methods.

6 Discussion and Conclusion

Limitation and Future Work There are two limitations for A*Net. (1) In the inductive setting, A*Net matches the performance of the purely path-based version of NBFNet, but fails to match the

performance of the original NBFNet. Future works may incorporate information beyond paths to fill this gap. (2) A*Net is focused on algorithm design rather than system design. As a result, the improvement in time and memory cost is less than the improvement in the number of messages. In the future, we will co-design the algorithm and the system to further improve the efficiency.

Societal Impact This work proposes an efficient model for path-based reasoning on knowledge graphs. On one hand, this work reduces the training and test time of reasoning models, which helps control carbon emission. On the other hand, reasoning models might be used in malicious activities, such as discovering sensitive relationship in anonymized data. The misuse potential of reasoning models increases as the quality of the reasoning model improves.

Conclusion In this work, we propose A*Net to efficiently learn path-based methods for knowledge graph reasoning. We show that the important paths in path-based methods can be efficiently computed via the A* algorithm, which uses a priority function to prioritize propagation towards important paths. To have a good priority function for efficient reasoning, we devise a neural priority function and jointly learn the priority function and propagation for path-based reasoning. Experiments on both transductive and inductive knowledge graph reasoning demonstrate that A*Net speeds up existing state-of-the-art path-based methods significantly, with negligible drop in performance.

References

- [1] Mattia Atzeni, Jasmina Bogojenska, and Andreas Loukas. Sqaler: Scaling question answering by decoupling multi-hop and logical reasoning. *Advances in Neural Information Processing Systems*, 34, 2021.
- [2] Yushi Bai, Zhitao Ying, Hongyu Ren, and Jure Leskovec. Modeling heterogeneous hierarchies with relation-specific hyperbolic cones. *Advances in Neural Information Processing Systems*, 34, 2021.
- [3] Richard Bellman. On a routing problem. *Quarterly of applied mathematics*, 16(1):87–90, 1958.
- [4] Jonathan Berant, Andrew Chou, Roy Frostig, and Percy Liang. Semantic parsing on freebase from question-answer pairs. In *Proceedings of the 2013 conference on empirical methods in natural language processing*, pages 1533–1544, 2013.
- [5] Antoine Bordes, Nicolas Usunier, Alberto Garcia-Duran, Jason Weston, and Oksana Yakhnenko. Translating embeddings for modeling multi-relational data. *Advances in neural information processing systems*, 26, 2013.
- [6] Ines Chami, Adva Wolf, Da-Cheng Juan, Frederic Sala, Sujith Ravi, and Christopher Ré. Low-dimensional hyperbolic knowledge graph embeddings. In *Proceedings of the 58th Annual Meeting of the Association for Computational Linguistics*, pages 6901–6914, 2020.
- [7] Jie Chen, Tengfei Ma, and Cao Xiao. Fastgcn: Fast learning with graph convolutional networks via importance sampling. In *International Conference on Learning Representations*, 2018.
- [8] Ming Chen, Zhewei Wei, Bolin Ding, Yaliang Li, Ye Yuan, Xiaoyong Du, and Ji-Rong Wen. Scalable graph neural networks via bidirectional propagation. *Advances in neural information processing systems*, 33:14556–14566, 2020.
- [9] Wenhui Chen, Wenhan Xiong, Xifeng Yan, and William Yang Wang. Variational knowledge graph reasoning. In *Proceedings of the 2018 Conference of the North American Chapter of the Association for Computational Linguistics: Human Language Technologies, Volume 1 (Long Papers)*, pages 1823–1832, 2018.
- [10] Gabriele Corso, Luca Cavalleri, Dominique Beaini, Pietro Liò, and Petar Veličković. Principal neighbourhood aggregation for graph nets. *Advances in Neural Information Processing Systems*, 33:13260–13271, 2020.
- [11] Rajarshi Das, Shehzaad Dhuliawala, Manzil Zaheer, Luke Vilnis, Ishan Durugkar, Akshay Krishnamurthy, Alex Smola, and Andrew McCallum. Go for a walk and arrive at the answer: Reasoning over paths in knowledge bases using reinforcement learning. In *International Conference on Learning Representations*, 2018.
- [12] Rajarshi Das, Arvind Neelakantan, David Belanger, and Andrew McCallum. Chains of reasoning over entities, relations, and text using recurrent neural networks. In *Proceedings of the 15th*

- Conference of the European Chapter of the Association for Computational Linguistics: Volume 1, Long Papers*, pages 132–141, 2017.
- [13] Tim Dettmers, Pasquale Minervini, Pontus Stenetorp, and Sebastian Riedel. Convolutional 2d knowledge graph embeddings. In *Proceedings of the AAAI Conference on Artificial Intelligence*, volume 32, 2018.
 - [14] Arthur Feeney, Rishabh Gupta, Veronika Thost, Rico Angell, Gayathri Chandu, Yash Adhikari, and Tengfei Ma. Relation matters in sampling: A scalable multi-relational graph neural network for drug-drug interaction prediction. *arXiv preprint arXiv:2105.13975*, 2021.
 - [15] Fabrizio Frasca, Emanuele Rossi, Davide Eynard, Ben Chamberlain, Michael Bronstein, and Federico Monti. Sign: Scalable inception graph neural networks. *arXiv preprint arXiv:2004.11198*, 2020.
 - [16] Matt Gardner and Tom Mitchell. Efficient and expressive knowledge base completion using subgraph feature extraction. In *Proceedings of the 2015 Conference on Empirical Methods in Natural Language Processing*, pages 1488–1498, 2015.
 - [17] Ben Goertzel and Cassio Pennachin. *Artificial general intelligence*, volume 2. Springer, 2007.
 - [18] Will Hamilton, Zitao Ying, and Jure Leskovec. Inductive representation learning on large graphs. *Advances in neural information processing systems*, 30, 2017.
 - [19] Peter E Hart, Nils J Nilsson, and Bertram Raphael. A formal basis for the heuristic determination of minimum cost paths. *IEEE transactions on Systems Science and Cybernetics*, 4(2):100–107, 1968.
 - [20] Udo Hebisch and Hanns Joachim Weinert. *Semirings: algebraic theory and applications in computer science*, volume 5. World Scientific, 1998.
 - [21] Marcel Hildebrandt, Jorge Andres Quintero Serna, Yunpu Ma, Martin Ringsquandl, Mitchell Joblin, and Volker Tresp. Reasoning on knowledge graphs with debate dynamics. In *Proceedings of the AAAI Conference on Artificial Intelligence*, volume 34, pages 4123–4131, 2020.
 - [22] Wenbing Huang, Tong Zhang, Yu Rong, and Junzhou Huang. Adaptive sampling towards fast graph representation learning. *Advances in neural information processing systems*, 31, 2018.
 - [23] Johannes Klicpera, Aleksandar Bojchevski, and Stephan Günnemann. Predict then propagate: Graph neural networks meet personalized pagerank. In *International Conference on Learning Representations*, 2018.
 - [24] Ni Lao and William W Cohen. Relational retrieval using a combination of path-constrained random walks. *Machine learning*, 81(1):53–67, 2010.
 - [25] Xi Victoria Lin, Richard Socher, and Caiming Xiong. Multi-hop knowledge graph reasoning with reward shaping. In *EMNLP*, 2018.
 - [26] John W Lloyd. *Foundations of logic programming*. Springer Science & Business Media, 2012.
 - [27] Arvind Neelakantan, Benjamin Roth, and Andrew McCallum. Compositional vector space models for knowledge base completion. In *Proceedings of the 53rd Annual Meeting of the Association for Computational Linguistics and the 7th International Joint Conference on Natural Language Processing (Volume 1: Long Papers)*, pages 156–166, 2015.
 - [28] Judea Pearl. *Probabilistic reasoning in intelligent systems: networks of plausible inference*. Morgan kaufmann, 1988.
 - [29] Meng Qu, Junkun Chen, Louis-Pascal Xhonneux, Yoshua Bengio, and Jian Tang. Rnnlogic: Learning logic rules for reasoning on knowledge graphs. In *International Conference on Learning Representations*, 2021.
 - [30] Ali Sadeghian, Mohammadreza Armandpour, Patrick Ding, and Daisy Zhe Wang. Drum: End-to-end differentiable rule mining on knowledge graphs. volume 32, pages 15347–15357, 2019.
 - [31] Michael Schlichtkrull, Thomas N Kipf, Peter Bloem, Rianne van den Berg, Ivan Titov, and Max Welling. Modeling relational data with graph convolutional networks. In *European semantic web conference*, pages 593–607. Springer, 2018.
 - [32] Yelong Shen, Jianshu Chen, Po-Sen Huang, Yuqing Guo, and Jianfeng Gao. M-walk: Learning to walk over graphs using monte carlo tree search. *Advances in Neural Information Processing Systems*, 31, 2018.

- [33] Zhiqing Sun, Zhi-Hong Deng, Jian-Yun Nie, and Jian Tang. Rotate: Knowledge graph embedding by relational rotation in complex space. In *International Conference on Learning Representations*, 2019.
- [34] Komal Teru, Etienne Denis, and Will Hamilton. Inductive relation prediction by subgraph reasoning. In *International Conference on Machine Learning*, pages 9448–9457. PMLR, 2020.
- [35] Kristina Toutanova and Danqi Chen. Observed versus latent features for knowledge base and text inference. In *Proceedings of the 3rd workshop on continuous vector space models and their compositionality*, pages 57–66, 2015.
- [36] Kristina Toutanova, Xi Victoria Lin, Wen-tau Yih, Hoifung Poon, and Chris Quirk. Compositional learning of embeddings for relation paths in knowledge base and text. In *Proceedings of the 54th Annual Meeting of the Association for Computational Linguistics (Volume 1: Long Papers)*, pages 1434–1444, 2016.
- [37] Shikhar Vashishth, Soumya Sanyal, Vikram Nitin, and Partha Talukdar. Composition-based multi-relational graph convolutional networks. In *International Conference on Learning Representations*, 2020.
- [38] Hongwei Wang, Hongyu Ren, and Jure Leskovec. Relational message passing for knowledge graph completion. In *Proceedings of the 27th ACM SIGKDD Conference on Knowledge Discovery & Data Mining*, pages 1697–1707, 2021.
- [39] Felix Wu, Amauri Souza, Tianyi Zhang, Christopher Fifty, Tao Yu, and Kilian Weinberger. Simplifying graph convolutional networks. In *International conference on machine learning*, pages 6861–6871. PMLR, 2019.
- [40] Wenhan Xiong, Thien Hoang, and William Yang Wang. Deeppath: A reinforcement learning method for knowledge graph reasoning. In *Proceedings of the 2017 Conference on Empirical Methods in Natural Language Processing (EMNLP 2017)*, Copenhagen, Denmark, September 2017. ACL.
- [41] Xiaoran Xu, Wei Feng, Yunsheng Jiang, Xiaohui Xie, Zhiqing Sun, and Zhi-Hong Deng. Dynamically pruned message passing networks for large-scale knowledge graph reasoning. In *International Conference on Learning Representations*, 2019.
- [42] Bishan Yang, Wen-tau Yih, Xiaodong He, Jianfeng Gao, and Li Deng. Embedding entities and relations for learning and inference in knowledge bases. *International Conference on Learning Representations*, 2015.
- [43] Fan Yang, Zhilin Yang, and William W Cohen. Differentiable learning of logical rules for knowledge base reasoning. In *Advances in Neural Information Processing Systems*, pages 2316–2325, 2017.
- [44] Hanqing Zeng, Hongkuan Zhou, Ajitesh Srivastava, Rajgopal Kannan, and Viktor Prasanna. Graphsaint: Graph sampling based inductive learning method. In *International Conference on Learning Representations*, 2019.
- [45] Fuzheng Zhang, Nicholas Jing Yuan, Defu Lian, Xing Xie, and Wei-Ying Ma. Collaborative knowledge base embedding for recommender systems. In *Proceedings of the 22nd ACM SIGKDD international conference on knowledge discovery and data mining*, pages 353–362, 2016.
- [46] Yongqi Zhang and Quanming Yao. Knowledge graph reasoning with relational digraph. In *Proceedings of the ACM Web Conference 2022*, pages 912–924, 2022.
- [47] Zhanqiu Zhang, Jianyu Cai, Yongdong Zhang, and Jie Wang. Learning hierarchy-aware knowledge graph embeddings for link prediction. In *Proceedings of the AAAI Conference on Artificial Intelligence*, volume 34, pages 3065–3072, 2020.
- [48] Zhaocheng Zhu, Chence Shi, Zuobai Zhang, Shengchao Liu, Minghao Xu, Xinyu Yuan, Yangtian Zhang, Junkun Chen, Huiyu Cai, Jiarui Lu, et al. Torchdrug: A powerful and flexible machine learning platform for drug discovery. *arXiv preprint arXiv:2202.08320*, 2022.
- [49] Zhaocheng Zhu, Zuobai Zhang, Louis-Pascal Xhonneux, and Jian Tang. Neural bellman-ford networks: A general graph neural network framework for link prediction. *Advances in Neural Information Processing Systems*, 34, 2021.

A Path-based Reasoning with A* Algorithm

Here we prove the correctness of path-based reasoning with A* algorithm.

A.1 Iterative Computation of a Superset of Important Paths

First, we prove that $\hat{\mathcal{P}}_{u \rightsquigarrow v|q}^{(t)}$ computed by Eqn. 6 and 7 equals to the set of important paths and paths that are different from important paths in the last hop.

Theorem 1. *If $m_q(P) : \mathcal{P} \mapsto \{0, 1\}$ can determine whether paths that begin with P contain any important path, the set of paths $\hat{\mathcal{P}}_{u \rightsquigarrow v|q}^{(t)}$ computed by Eqn. 6 and 7 equals to the set of important paths and paths that are different from important paths in the last hop of length t .*

$$\hat{\mathcal{P}}_{u \rightsquigarrow v|q}^{(0)} \leftarrow \{(u, \text{self loop}, v)\} \text{ if } u = v \text{ else } \emptyset \quad (6)$$

$$\hat{\mathcal{P}}_{u \rightsquigarrow v|q}^{(t)} \leftarrow \bigcup_{(x,r,v) \in \mathcal{E}(v)} \left\{ \text{concat}(P, \{(x, r, v)\}) \mid P \in \hat{\mathcal{P}}_{u \rightsquigarrow x|q}^{(t-1)}, m_q(P) = 1 \right\} \quad (7)$$

Proof. We use $\mathcal{Q}_{u \rightsquigarrow v|q}^{(t)}$ to denote the set of important paths and paths that are different from important paths in the last hop of length t . For paths of length 0, we define them to be important as they should be the prefix of some important paths. Therefore, $\mathcal{Q}_{u \rightsquigarrow v|q}^{(0)} = \{(u, \text{self loop}, v)\}$ if $u = v$ else \emptyset . We use $P_{:-1}$ to denote the prefix of path P without the last hop. The goal is to prove $\hat{\mathcal{P}}_{u \rightsquigarrow v|q}^{(t)} = \mathcal{Q}_{u \rightsquigarrow v|q}^{(t)}$.

First, we prove $\hat{\mathcal{P}}_{u \rightsquigarrow v|q}^{(t)} \subseteq \mathcal{Q}_{u \rightsquigarrow v|q}^{(t)}$. It is obvious that $\hat{\mathcal{P}}_{u \rightsquigarrow v|q}^{(0)} \subseteq \mathcal{Q}_{u \rightsquigarrow v|q}^{(0)}$. In the case of $t > 0$, $\forall P \in \hat{\mathcal{P}}_{u \rightsquigarrow v|q}^{(t)}$, we have $m_q(P_{:-1}) = 1$ according to Eqn. 7. Therefore, $P \in \mathcal{Q}_{u \rightsquigarrow v|q}^{(t)}$.

Second, we prove $\mathcal{Q}_{u \rightsquigarrow v|q}^{(t)} \subseteq \hat{\mathcal{P}}_{u \rightsquigarrow v|q}^{(t)}$ by induction. For the base case $t = 0$, it is obvious that $\mathcal{Q}_{u \rightsquigarrow v|q}^{(0)} \subseteq \hat{\mathcal{P}}_{u \rightsquigarrow v|q}^{(0)}$. For the inductive case $t > 0$, $\forall Q \in \mathcal{Q}_{u \rightsquigarrow v|q}^{(t)}$, we have $Q_{:-1} \in \mathcal{Q}_{u \rightsquigarrow v|q}^{(t-1)}$ and $m_q(Q_{:-1}) = 1$ according to the definition of $\mathcal{Q}_{u \rightsquigarrow v|q}^{(t)}$. Based on the inductive assumption, we get $Q_{:-1} \in \hat{\mathcal{P}}_{u \rightsquigarrow v|q}^{(t-1)}$. Therefore, $Q \in \hat{\mathcal{P}}_{u \rightsquigarrow v|q}^{(t)}$ according to Eqn. 7. \square

As a corollary of Thm. 1, $\hat{\mathcal{P}}_{u \rightsquigarrow v|q}$ is a slightly larger superset of the important paths $\mathcal{P}_{u \rightsquigarrow v|q}$.

Corollary 1. *If the end nodes of important paths are uniformly distributed in the knowledge graph, the expected size of $\hat{\mathcal{P}}_{u \rightsquigarrow v|q}^{(t)}$ is $|\mathcal{P}_{u \rightsquigarrow v|q}^{(t)}| + \frac{|\mathcal{E}|}{|\mathcal{V}|} |\mathcal{P}_{u \rightsquigarrow v|q}^{(t-1)}|$.*

Proof. Thm. 1 indicates that $\hat{\mathcal{P}}_{u \rightsquigarrow v|q}^{(t)}$ contains two types of paths: important paths and paths that are different from important paths in the last hop of length t . The number of the first type is $|\mathcal{P}_{u \rightsquigarrow v|q}^{(t)}|$. Each of the second type corresponds to an important path of length $t - 1$. From an inverse perspective, each important path of length $t - 1$ generates d paths of the second type for $\hat{\mathcal{P}}_{u \rightsquigarrow v|q}^{(t)}$, where d is the degree of the end node in the path. If the end nodes are uniformly distributed in the knowledge graph, we have $\mathbb{E}[\hat{\mathcal{P}}_{u \rightsquigarrow v|q}^{(t)}] = |\mathcal{P}_{u \rightsquigarrow v|q}^{(t)}| + \frac{|\mathcal{E}|}{|\mathcal{V}|} |\mathcal{P}_{u \rightsquigarrow v|q}^{(t-1)}|$. For real-world knowledge graphs, $\frac{|\mathcal{E}|}{|\mathcal{V}|}$ is usually a small constant (e.g., ≤ 50), and $|\hat{\mathcal{P}}_{u \rightsquigarrow v|q}^{(t)}|$ is slightly larger than $|\mathcal{P}_{u \rightsquigarrow v|q}^{(t)}|$ in terms of complexity. \square

A.2 From Tree Search to Dynamic Programming

Second, we demonstrate that Eqn. 7 can be solved by Eqn. 8 if paths with the same length and the same stop node can be merged.

Proposition 1. If $m_q(P)$ only depends on the length of the path t , the start node u and the end node x , by replacing $m_q(P)$ with $s_{uq}^{(t)}(x)$, $\hat{\mathcal{P}}_{u \rightsquigarrow v|q}^{(t)}$ can be computed as follows

$$\hat{\mathcal{P}}_{u \rightsquigarrow v|q}^{(t)} \leftarrow \bigcup_{x \in \mathcal{V}, s_{uq}^{(t-1)}(x)=1, (x,r,v) \in \mathcal{E}(v)} \left\{ \text{concat}(P, \{(x, r, v)\}) \mid P \in \hat{\mathcal{P}}_{u \rightsquigarrow x|q}^{(t-1)} \right\} \quad (8)$$

This proposition is obvious. As a result of Prop. 1, we merge paths by their length and stop nodes, which turns the exponential tree search to a polynomial dynamic programming algorithm.

A.3 Reasoning with A* Algorithm

Finally, we prove that the A* iteration (Eqn. 9) covers all important paths for reasoning (Eqn. 5).

Theorem 2. If $s_{uq}^{(t)}(x) : \mathcal{V} \mapsto \{0, 1\}$ can determine whether paths from u to x are important or not, and (\oplus, \otimes) forms a semiring [20], the representation $\mathbf{h}_q(u, v)$ for path-based reasoning can be computed by

$$\mathbf{h}_q^{(t)}(u, v) \leftarrow \left(\bigoplus_{x \in \mathcal{V}, s_{uq}^{(t-1)}(x)=1, (x,r,v) \in \mathcal{E}(v)} \mathbf{h}_q^{(t-1)}(u, x) \otimes \mathbf{w}_q(x, r, v) \right) \oplus \mathbf{h}_q^{(0)}(u, v) \quad (9)$$

Proof. In order to prove Thm. 2, we first prove a lemma for the analytic form of $\mathbf{h}_q^{(t)}(u, v)$, and then show that $\lim_{t \rightarrow \infty} \mathbf{h}_q^{(t)}(u, v)$ converges to the goal of path-based reasoning.

Lemma 1. Under the same condition as Thm. 2, the intermediate representation $\mathbf{h}_q^{(t)}(u, v)$ computed by Eqn. 2 and 9 aggregates all important paths within a length of t edges, i.e.

$$\mathbf{h}_q^{(t)}(u, v) = \bigoplus_{P \in \hat{\mathcal{P}}_{u \rightsquigarrow v|q}^{(\leq t)}} \bigotimes_{i=1}^{|P|} \mathbf{w}_q(e_i) \quad (14)$$

where $\hat{\mathcal{P}}_{u \rightsquigarrow v|q}^{(\leq t)} = \bigcup_{k=0}^t \hat{\mathcal{P}}_{u \rightsquigarrow v|q}^{(k)}$.

Proof. We prove Lem. 1 by induction. Let $\mathbb{0}_q$ and $\mathbb{1}_q$ denote the identity elements of \oplus and \otimes respectively. We have $\mathbb{1}_q(u = v) = \mathbb{1}_q$ if $u = v$ else $\mathbb{0}_q$. Note paths of length 0 only contain self loops, and we define them as important paths, since they should be prefix of some important paths.

For the base case $t = 0$, we have $\mathbf{h}_q^{(0)}(u, u) = \mathbb{1}_q = \bigoplus_{P \in \mathcal{P}_{u \rightsquigarrow u|q} : |P| \leq 0} \bigotimes_{i=1}^{|P|} \mathbf{w}_q(e_i)$ since the only path from u to u is the self loop, which has the representation $\mathbb{1}_q$. For $u \neq v$, we have $\mathbf{h}_q^{(0)}(u, v) = \mathbb{0}_q = \bigoplus_{P \in \mathcal{P}_{u \rightsquigarrow v|q} : |P| \leq 0} \bigotimes_{i=1}^{|P|} \mathbf{w}_q(e_i)$ since there is no important path from u to v within length 0.

For the inductive case $t > 0$, we have

$$\mathbf{h}_q^{(t)}(u, v) = \left(\bigoplus_{\substack{s_{uq}^{(t-1)}(x)=1 \\ (x,r,v) \in \mathcal{E}(v)}} \mathbf{h}_q^{(t-1)}(u, x) \otimes \mathbf{w}_q(x, r, v) \right) \oplus \mathbf{h}_q^{(0)}(u, v) \quad (15)$$

$$= \left[\bigoplus_{\substack{s_{uq}^{(t-1)}(x)=1 \\ (x,r,v) \in \mathcal{E}(v)}} \left(\bigoplus_{\hat{\mathcal{P}}_{u \rightsquigarrow x|q}^{(\leq t-1)}} \bigotimes_{i=1}^{|P|} \mathbf{w}_q(e_i) \right) \otimes \mathbf{w}_q(x, r, v) \right] \oplus \mathbf{h}_q^{(0)}(u, v) \quad (16)$$

$$= \left\{ \bigoplus_{\substack{s_{uq}^{(t-1)}(x)=1 \\ (x,r,v) \in \mathcal{E}(v)}} \left[\bigoplus_{\hat{\mathcal{P}}_{u \rightsquigarrow x|q}^{(\leq t-1)}} \left(\bigotimes_{i=1}^{|P|} \mathbf{w}_q(e_i) \right) \otimes \mathbf{w}_q(x, r, v) \right] \right\} \oplus \mathbf{h}_q^{(0)}(u, v) \quad (17)$$

$$= \left(\bigoplus_{P \in \hat{\mathcal{P}}_{u \rightsquigarrow v|q}^{(\leq t)} \setminus \hat{\mathcal{P}}_{u \rightsquigarrow v|q}^{(0)}} \bigotimes_{i=1}^{|P|} \mathbf{w}_q(e_i) \right) \oplus \left(\bigoplus_{P \in \hat{\mathcal{P}}_{u \rightsquigarrow v|q}^{(0)}} \bigotimes_{i=1}^{|P|} \mathbf{w}_q(e_i) \right) \quad (18)$$

$$= \bigoplus_{P \in \hat{\mathcal{P}}_{u \rightsquigarrow v|q}: |P| \leq t} \bigotimes_{i=1}^{|P|} \mathbf{w}_q(e_i), \quad (19)$$

where Eqn. 16 uses the inductive assumption, Eqn. 17 relies on the distributive property of \otimes over \oplus , and Eqn. 18 uses Prop. 1. In the above equations, \bigotimes and \otimes are always applied before \bigoplus and \oplus . \square

Since $\mathcal{P}_{u \rightsquigarrow v|q}^{(t)} \subseteq \hat{\mathcal{P}}_{u \rightsquigarrow v|q}^{(t)}$, we have $\mathcal{P}_{u \rightsquigarrow v|q} \subseteq \hat{\mathcal{P}}_{u \rightsquigarrow v|q} \subseteq \mathcal{P}_{u \rightsquigarrow v}$. Based on Lem. 1 and Eqn. 5, it is obvious to see that

$$\lim_{t \rightarrow \infty} \mathbf{h}_q^{(t)}(u, v) = \bigoplus_{P \in \hat{\mathcal{P}}_{u \rightsquigarrow v|q}} \mathbf{h}_q(P) \approx \bigoplus_{P \in \mathcal{P}_{u \rightsquigarrow v}} \mathbf{h}_q(P) = \mathbf{h}_q(u, v) \quad (20)$$

Therefore, Thm. 2 holds. \square

B Additional Edge Selection Step in A*Net

As demonstrated in Sec. 3.2, A*Net selects top- K nodes according to the current priority function, and computes the A* iteration

$$\mathbf{h}_q^{(t)}(u, v) \leftarrow \left(\bigoplus_{x \in \mathcal{X}^{(t)}, (x, r, v) \in \mathcal{E}(v)} s_{uq}^{(t-1)}(x) \left(\mathbf{h}_q^{(t-1)}(u, x) \otimes \mathbf{w}_q(x, r, v) \right) \right) \oplus \mathbf{h}_q^{(0)}(u, v) \quad (11)$$

However, even if we choose a small K , Eqn. 11 may still propagate the messages to many nodes in the knowledge graph, resulting in a high computation cost. This is because some nodes in the knowledge graph may have very large degrees, e.g., the entity *Human* is connected to every person in the knowledge graph. In fact, it is not necessary to propagate the messages to every neighbor of a node, especially if the node has a large degree. Based on this observation, we propose to further select top- L edges from the neighborhood of $\mathcal{X}^{(t)}$ to create $\mathcal{E}^{(t)}$

$$\mathcal{E}^{(t)} \leftarrow \text{TopL}(s_{uq}^{(t-1)}(v) | x \in \mathcal{X}^{(t)}, (x, r, v) \in \mathcal{E}(x)) \quad (21)$$

where each edge is picked according to the priority of node v , i.e., the tail node of an edge. By doing so, we reuse the neural priority function and avoid introducing any additional priority function. The intuition of Eqn. 21 is that if an edge (x, r, v) goes to a node with a higher priority, it is likely we are propagating towards the answer entities. With the selected edges $\mathcal{E}^{(t)}$, the A* iteration becomes

$$\mathbf{h}_q^{(t)}(u, v) \leftarrow \left(\bigoplus_{x \in \mathcal{X}^{(t)}, (x, r, v) \in \mathcal{E}^{(t)}(v)} s_{uq}^{(t-1)}(x) \left(\mathbf{h}_q^{(t-1)}(u, x) \otimes \mathbf{w}_q(x, r, v) \right) \right) \oplus \mathbf{h}_q^{(0)}(u, v) \quad (22)$$

which is also the implementation in Alg. 1.

C Padding-Free Operations

In A*Net, different training samples may have very different sizes for the selected nodes $\mathcal{V}^{(t)}$ and $\mathcal{E}^{(t)}$. To avoid the additional computation over padding in conventional batched execution, we introduce padding-free operations, which operates on the concatenation of samples without any padding.

Specifically, padding-free operations add an offset for each sample in the batch, such that we can distinguish different samples when we apply operations to the whole batch. As showed in Fig. 6, for a padding-free *topk*, we first add the offsets 0 and 4 for two samples, and then apply a sort operation over the whole batch. Since the offset ensures that elements in the later sample are always larger than elements in the former sample, the order of the samples are naturally preserved after the sort operation. We then apply indexing operations and remove the offsets to get the correct output.

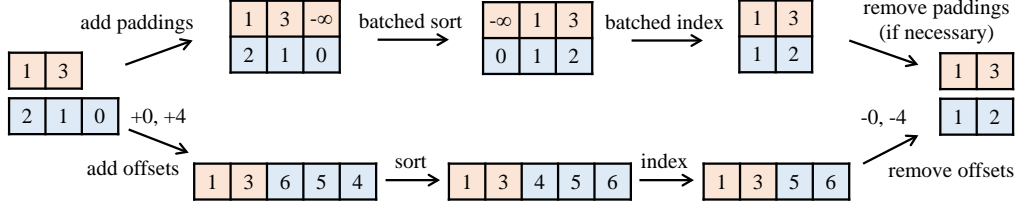


Figure 6: Comparison between padding-based *topk* (up) and padding-free *topk* (down) for $K = 2$. Padding-based operations first add paddings to create a padded tensor for batched operations, and then remove the paddings. Padding-free operations add offsets to distinguish different samples (showed in colors), apply single-sample operations, and then remove the offsets.

Based on the above idea, we implement padding-free *topk* for selecting nodes (Alg. 1 Line 6) and edges (Alg. 1 Line 9) in A*Net, and padding-free *unique* for computing the union of node sets (Alg. 1 Line 10). Alg. 2 and 3 provide the pseudo code for padding-free *topk* and *unique* respectively.

Algorithm 2 Padding-free implementation of *topk* in PyTorch

Input: Input values of each sample *inputs*, size of each sample *sizes*, K

Output: TopK values of each sample, indices of topk values

```

1 offset = inputs.max() - inputs.min() + 1
2 # the sample id of each element
3 sample_ids = torch.arange(batch_size).repeat_interleave(sizes)
4 inputs = inputs + offset * sample_ids
5 sorteds, indices = inputs.sort()
6 sorteds = sorteds - offset * sample_ids
7 ranges = torch.arange(K).repeat(batch_size)
8 ranges = ranges + sizes.cumsum(0).repeat_interleave(K) - K
9 return sorteds[ranges], indices[ranges]
```

Algorithm 3 Padding-free implementation of *unique* in PyTorch

Input: Input values of each sample *inputs*, size of each sample *sizes*

Output: Unique values of each sample, number of unique values in each sample

```

1 offset = inputs.max() - inputs.min() + 1
2 # the sample id of each element
3 sample_ids = torch.arange(batch_size).repeat_interleave(sizes)
4 inputs = inputs + offset * sample_ids
5 uniques = inputs.unique()
6 sample_ids = uniques // offset
7 uniques = uniques % offset
8 sizes = sample_ids.bincount(maxlength=batch_size)
9 return uniques, sizes
```

D Datasets & Evaluation

Dataset statistics for transductive and inductive knowledge graph reasoning is summarized in Tab. 5 and 6 respectively. For the transductive setting, given a head (or tail) and a query relation, we rank each answer tail (or head) entity against all negative entities. For the inductive setting, we follow the setting in [34] and rank each each answer tail (or head) entity against 50 randomly sampled negative entities. We report the mean reciprocal rank (MRR) and HITS at K (H@K) of the rankings.

As for efficiency evaluation, we compute the number of messages (#message) per layer, wall time per epoch and memory cost. The number of messages is averaged over all samples and layers

$$\text{\#message} = \mathbb{E}_{(u,q,v) \in \mathcal{E}} \mathbb{E}_t \left| \mathcal{E}^{(t)} \right| \quad (23)$$

Table 5: Dataset statistics for transductive knowledge graph reasoning.

Dataset	#Relation	#Entity	#Triplet		
			#Train	#Valid	#Test
FB15k-237 [35]	237	14,541	272,115	17,535	20,466
WN18RR [13]	11	40,943	86,835	3,034	3,134

Table 6: Dataset statistics for inductive knowledge graph reasoning.

Dataset		#Relation	Train			Validation			Test	
			#Entity	#Query	#Fact	#Entity	#Query	#Fact	#Entity	#Query
FB15k-237 [34]	v1	180	1,594	4,245	4,245	1,594	489	4,245	1,093	205
	v2	200	2,608	9,739	9,739	2,608	1,166	9,739	1,660	478
	v3	215	3,668	17,986	17,986	3,668	2,194	17,986	2,501	865
	v4	219	4,707	27,203	27,203	4,707	3,352	27,203	3,051	1,424
WN18RR [34]	v1	9	2,746	5,410	5,410	2,746	630	5,410	922	188
	v2	10	6,954	15,262	15,262	6,954	1,838	15,262	2,757	441
	v3	11	12,078	25,901	25,901	12,078	3,097	25,901	5,084	605
	v4	9	3,861	7,940	7,940	3,861	934	7,940	7,084	1,429

The wall time per epoch is defined as the average time to complete a single training epoch. We measure the wall time based on 10 epochs. The memory cost is measured by the function `torch.cuda.max_memory_allocated()` in PyTorch.

E Implementation Details

Our work is based on the open-source codebase of path-based reasoning with Bellman-Ford algorithm⁴. Tab. 7 and 8 list the hyperparameters for model architectures and selection ratios respectively. We keep the same model for all splits of a dataset, and only tune the ratios for different splits.

Table 7: Hyperparameters for model architecture and training. All the hyperparameters are kept the same as NBFNet [49], except for the neural priority function introduced in A*Net.

Hyperparameter		FB15k-237	WN18RR
Message Passing	#step (T)	6	6
	hidden dim.	32	32
Priority Function	$g(\cdot)$ #layer	1	1
	$f(\cdot)$ #layer	2	2
	hidden dim.	32	32
Learning	optimizer	Adam	Adam
	batch size	256	256
	learning rate	5e-3	5e-3
	#epoch	20	20
	adv. temperature	0.5	1
	#negative	32	32

Table 8: Hyperparameters for node selection and edge selection.

Hyperparameter		FB15k-237					WN18RR				
		transductive	v1	v2	v3	v4	transductive	v1	v2	v3	v4
Ratio	$K/ \mathcal{V} $	10%	50%	50%	20%	20%	1%	10%	2%	20%	1%
	$D \mathcal{V} / \mathcal{E} $	100%	100%	71%	100%	100%	100%	100%	100%	100%	100%

Neural Priority Function We parameterize the neural priority function $s_{uq}^{(t)}(x)$ in A*Net as follows

$$s_{uq}^{(t)}(x) = \sigma(f(\mathbf{h}_q^{(t)}(u, x) \otimes g([\mathbf{h}_q^{(t)}(u, x), \mathbf{q}])) \quad (24)$$

⁴<https://github.com/DeepGraphLearning/NBFNet>. MIT license.

where $f(\cdot)$ and $g(\cdot)$ are two feed-forward networks and σ is the sigmoid function. $g(\cdot)$ transforms the concatenation of $\mathbf{h}_q^{(t)}(u, x)$ and \mathbf{q} into a representation of the same shape as $\mathbf{h}_q^{(t)}(u, x)$, and $f(\cdot)$ maps the representation to a scalar.

Parameterization For a fair comparison with existing path-based methods, we follow NBFNet [49] and parameterize \oplus with principal neighborhood aggregation (PNA), which is a permutation-invariant function over a set of elements. We parameterize \otimes with the relation operation from DistMult [42], i.e., vector multiplication. Note that PNA relies on the degree information of each node to perform aggregation. We observe that PNA does not generalize well when degrees are dynamically determined by the priority function. Therefore, we precompute the degree for each node on the full graph, and use them in PNA no matter how many nodes and edges are selected by the priority function.

Data Augmentation We follow the data augmentation steps of NBFNet [49]. For each triplet (x, r, y) , we add an inverse triplet (y, r^{-1}, x) to the knowledge graph, so that A*Net can propagate in both directions. Each triplet and its inverse may have different priority and are picked independently in the edge selection step. Since test queries are always missing in the test graph, we remove the edges of training queries during training to prevent the model from copying the input.

F Two Different Implementations of NBFNet

While NBFNet [49] proposes to solve path-based reasoning with the Bellman-Ford algorithm, there are two different ways to implement the Bellman-Ford algorithm. One way is to directly implement the Bellman-Ford algorithm for computing Eqn. 1 (Fig. 7(b)). The other one is to apply the Bellman-Ford algorithm over an equivalent form of Eqn. 1 (Fig. 7(a)). Both implementations are correct when the semiring assumption holds (e.g., in shortest path problems). However, they are different when we parameterize them with neural networks, as neural networks may not satisfy the semiring assumption.

F.1 Original Implementation (NBFNet (path+))

The original implementation of NBFNet leverages the semiring assumption of $\langle \oplus, \otimes \rangle$ and computes an equivalent form of Eqn. 1

$$\mathbf{h}_q(u, v) = \bigoplus_{P \in \mathcal{P}_{u \rightsquigarrow v}} \mathbf{h}_q(P) = \bigoplus_{P \in \mathcal{P}_{u \rightsquigarrow v}} \textcircled{1}_q \mathbf{h}_q(P) + \bigoplus_{\substack{x \in \mathcal{V} \setminus \{u\} \\ P \in \mathcal{P}_{x \rightsquigarrow v}}} \textcircled{0}_q \mathbf{h}_q(P) \triangleq \bigoplus_{\substack{x \in \mathcal{V} \\ P \in \mathcal{P}_{x \rightsquigarrow v}}} \hat{\mathbf{h}}_q(P) \quad (25)$$

where $\textcircled{0}_q$ and $\textcircled{1}_q$ are the identity elements of \oplus and \otimes respectively. $\hat{\mathbf{h}}_q(P)$ is an augmented path representation with $\hat{\mathbf{h}}_q(P) = \mathbf{h}_q(P)$ if P starts with the node u and $\textcircled{0}_q$ otherwise. Intuitively, this implementation not only computes the paths in $\mathcal{P}_{u \rightsquigarrow v}$ (black paths in Fig. 7), but also computes the additional paths in $\mathcal{P}_{x \rightsquigarrow v}$ for $\forall x \in \mathcal{V} \setminus \{u\}$ (orange paths in Fig. 7).

The advantage of NBFNet (path+) is that the propagation in Bellman-Ford iteration (Eqn. 3) can be easily implemented with a sparse adjacency matrix of the *fixed* full graph. As a result, it enjoys good parallel computation from deep learning frameworks, though it considers additional paths. However, it is not clear whether the additional paths contribute positively or negatively to the prediction, since they may not equal to $\textcircled{0}_q$ when learned by neural networks.

F.2 Re-implementation (NBFNet (path))

In this paper, we re-implement NBFNet to compute the precise set of paths $\mathcal{P}_{u \rightsquigarrow v}$ in Eqn. 1, which is more faithful to the definition of path-based reasoning. However, it is very challenging to implement

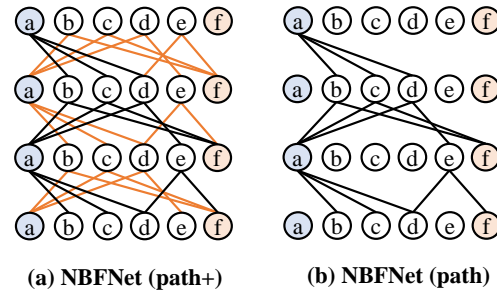


Figure 7: Comparison between NBFNet (path+) and NBFNet (path). (a) The original implementation, NBFNet (path+), aggregates additional paths (showed in colors) when predicting the answer entity. (b) Our re-implementation, NBFNet (path), only considers the paths in $\mathcal{P}_{a \rightsquigarrow f}$ for reasoning.

NBFNet (path). The reason is that at every iteration step, we need to construct a sparse adjacency matrix for a *dynamic* subgraph. For example, at the second iteration in Fig. 7(b), the subgraph contains the edges from $\{b, c, d\}$ to their neighbors. Moreover, different subgraphs should be constructed for different queries. To solve these challenges, we use the operations provided by TorchDrug [48] to efficiently construct the subgraphs and their adjacency matrices on-the-fly with GPUs.

In the main experiments of this paper, we mainly focus on comparing A*Net with NBFNet (path), since A*Net does not consider the additional paths like NBFNet (path+).

F.3 Performance Comparison

We compare the performance between NBFNet (path+) and NBFNet (path). As showed in Tab. 9, NBFNet (path) matches the performance of NBFNet (path+) in the transductive setting. This suggests the additional paths may not be important for reasoning in the transductive setting. However, Tab. 10 shows a gap between NBFNet (path+) and NBFNet (path). We conjecture the reason is that the additional path may be helpful in deciding the type of the tail entity v in the inductive setting.

Table 9: Performance of two NBFNet implementations on transductive knowledge graph reasoning.

Method	FB15k-237				WN18RR			
	MRR	H@1	H@3	H@10	MRR	H@1	H@3	H@10
NBFNet (path+)	0.415	0.321	0.454	0.599	0.551	0.497	0.573	0.666
NBFNet (path)	0.409	0.315	0.447	0.593	0.547	0.495	0.569	0.651

Table 10: Performance of two NBFNet implementations on inductive knowledge graph reasoning.

Method	FB15k-237				WN18RR			
	v1	v2	v3	v4	v1	v2	v3	v4
NBFNet (path+)	0.834	0.949	0.951	0.960	0.948	0.905	0.893	0.890
NBFNet (path)	0.697	0.871	0.910	0.907	0.877	0.822	0.720	0.802

G More Experiment Results

We provide the efficiency results on inductive knowledge graph reasoning in Tab. 11. It is observed that A*Net significantly reduces the number of messages compared to NBFNet (path) on both datasets and all splits. However, the wall time and memory cost are not reduced significantly. On some splits, e.g., FB15k-237 v2 and WN18RR v1, we observe that A*Net requires even more time and memory than NBFNet. This is because the training set of these splits are so small that the overhead of the neural priority function and node selection becomes the bottleneck. In the future, we will co-design the algorithm and the system to improve the time and memory cost in the inductive setting.

Table 11: Efficiency on inductive knowledge graph reasoning. V1-v4 refer to the 4 standard splits.

Method	v1			v2			v3			v4		
	#msg.	time	memory	#msg.	time	memory	#msg.	time	memory	#msg.	time	memory
FB15k-237												
NBFNet (path)	3,661	8.7 s	1.74 GiB	8,830	12.6 s	3.02 GiB	17,607	29.2 s	4.70 GiB	26,916	55.0 s	6.26 GiB
A*Net	2,203	18.8 s	575 MiB	6,814	14.2 s	3.84 GiB	4,719	24.8 s	4.10 GiB	7,301	42.0 s	5.23 GiB
Improvement	1.7×	0.46×	3.1×	1.3×	0.89×	0.79×	3.7×	1.2×	1.1×	3.7×	1.3×	1.2×
WN18RR												
NBFNet (path)	500	5.0 s	544 MiB	973	14.2 s	1.15 GiB	1,322	26.1 s	1.74 GiB	584	7.2 s	703 MiB
A*Net	316	5.7 s	647 MiB	248	15.9 s	846 MiB	1176	30.0 s	2.68 GiB	90	8.6 s	401 MiB
Improvement	1.6×	0.88×	0.84×	3.9×	0.89×	1.39×	1.1×	0.87×	0.65×	6.5×	0.84×	1.8×

H More Visualization of Learned Important Paths

Fig. 8 visualizes learned important paths on different samples. All the samples are picked from the test set of transductive FB15k-237.

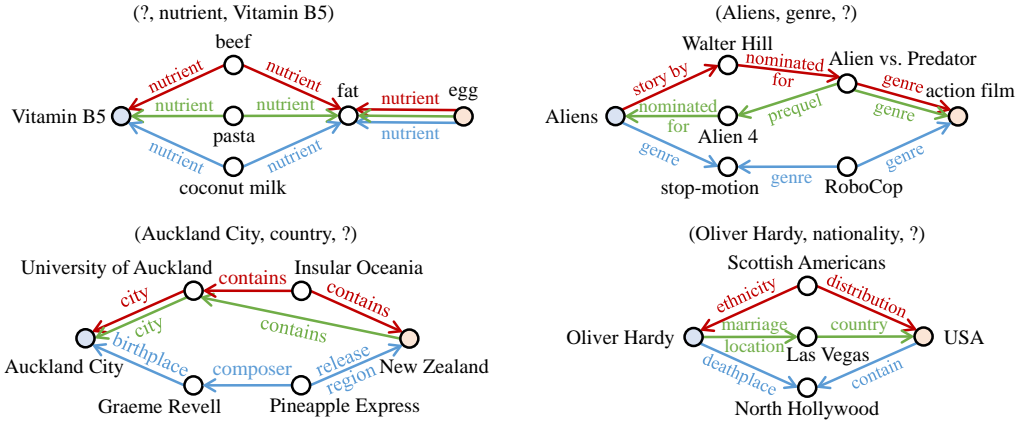


Figure 8: Visualization of important paths in A*Net on different test samples. Each important path is highlighted by a separate color.